

# ELTD1 deletion reduces vascular abnormality and improves T-cell recruitment after PD-1 blockade in glioma

Hua Huang, Maria Georganaki, Lei Liu Conze, Bàrbara Laviña, Luuk van Hooren, Kalyani Vemuri, Tiarne van de Walle, Mohanraj Ramachandran, Lei Zhang, Fredrik Pontén, Michael Bergqvist, Anja Smits, Christer Betsholtz, Elisabetta Dejana, Peetra U. Magnusson, Liqun He, Roberta Lugano, and Anna Dimberg

*Department of Immunology, Genetics and Pathology, The Rudbeck Laboratory, Science for Life Laboratory, Uppsala University, Uppsala, Sweden (H.H., M.G., L.L.C., B.L., L.v.H., K.V., T.v.d.W., M.R., FP, C.B., E.D., P.U.M., L.H., R.L., A.D.); Key Laboratory of Ministry of Education for Medicinal Plant Resource and Natural Pharmaceutical Chemistry, National Engineering Laboratory for Resource Developing of Endangered Chinese Crude Drugs in Northwest of China, College of Life Sciences, Shaanxi Normal University, Xi'an, China (L.Z.); Center for Research and Development, Gävle Hospital, Uppsala University, Gävle, Sweden (M.B.); Department of Radiation Sciences and Oncology, Umeå University Hospital, Umeå, Sweden (M.B.); Department of Clinical Neuroscience, Sahlgrenska Academy, Institute of Neuroscience and Physiology, University of Gothenburg, Gothenburg, Sweden (A.S.)*

**Corresponding Author:** Anna Dimberg, PhD, Department of Immunology, Genetics and Pathology, The Rudbeck Laboratory, Uppsala University, 75185 Uppsala, Sweden ([anna.dimberg@igp.uu.se](mailto:anna.dimberg@igp.uu.se)).

## Abstract

**Background.** Tumor vessels in glioma are molecularly and functionally abnormal, contributing to treatment resistance. Proteins differentially expressed in glioma vessels can change vessel phenotype and be targeted for therapy. ELTD1 (Adgrl4) is an orphan member of the adhesion G-protein-coupled receptor family upregulated in glioma vessels and has been suggested as a potential therapeutic target. However, the role of ELTD1 in regulating vessel function in glioblastoma is poorly understood.

**Methods.** ELTD1 expression in human gliomas and its association with patient survival was determined using tissue microarrays and public databases. The role of ELTD1 in regulating tumor vessel phenotype was analyzed using orthotopic glioma models and ELTD1<sup>-/-</sup> mice. Endothelial cells isolated from murine gliomas were transcriptionally profiled to determine differentially expressed genes and pathways. The consequence of ELTD1 deletion on glioma immunity was determined by treating tumor-bearing mice with PD-1-blocking antibodies.

**Results.** ELTD1 levels were upregulated in human glioma vessels, increased with tumor malignancy, and were associated with poor patient survival. Progression of orthotopic gliomas was not affected by ELTD1 deletion, however, tumor vascular function was improved in ELTD1<sup>-/-</sup> mice. Bioinformatic analysis of differentially expressed genes indicated increased inflammatory response and decreased proliferation in tumor endothelium in ELTD1<sup>-/-</sup> mice. Consistent with an enhanced inflammatory response, ELTD1 deletion improved T-cell infiltration in GL261-bearing mice after PD-1 checkpoint blockade.

**Conclusion.** Our data demonstrate that ELTD1 participates in inducing vascular dysfunction in glioma, and suggest that targeting of ELTD1 may normalize the vessels and improve the response to immunotherapy.

Glioblastomas (GBM) are malignant gliomas (WHO grade IV) characterized by nuclear atypia, high tumor cell proliferation, necrosis, microvascular proliferation, and pleomorphic vessels.<sup>1,2</sup> The vessels are dysfunctional and aggravate the

condition by inducing vasogenic edema and by supplying a niche for cancer stem cells.<sup>3</sup> In addition, dysfunctional vessels can reduce transport of anticancer drugs and may limit the response to cancer immunotherapy by giving rise

## Key Points

1. ELTD1 is elevated in glioma vessels and is associated with poor patient survival.
2. ELTD1 deletion improves vessel function in murine glioma models.
3. ELTD1 deletion improves T-cell recruitment in response to PD-1 checkpoint blockade in experimental glioma.

## Importance of the Study

High-grade gliomas are aggressive brain tumors characterized by a dysfunctional tumor vasculature that alters the microenvironment and hinders therapy. There is a need for identification of targets to improve vessel function and enable pharmaceutical targeting of glioma. Here, we demonstrate that the G-protein-coupled receptor ELTD1 regulates vascular function in glioma. ELTD1 is upregulated in tumor vessels in glioma, its levels positively correlating with tumor malignancy grade.

Orthotopic glioma growth is not affected by genetic knockout of ELTD1 in mice, but vascular dysfunction is reduced and the perfusion of the tumor is improved. Genes related to inflammation are more highly expressed in tumor endothelial cells in ELTD1<sup>-/-</sup> mice and T-cell recruitment is enhanced in response to PD-1 checkpoint blockade therapy. This study identifies ELTD1 as a potential target to improve vessel function and enhance the response to cancer immunotherapy in glioma.

to immunosuppression.<sup>4</sup> Lower-grade gliomas (LGGs) are classified into molecular subgroups depending on isocitrate dehydrogenase (IDH) mutational status and the presence/absence of 1p/19q co-deletion. IDH-mutated (IDHmut) 1p/19q codeleted tumors are classified as oligodendrogliomas, whereas IDHmut non-codeleted tumors are astrocytomas.<sup>5</sup> Gliomas with wildtype IDH are molecularly similar to primary GBM and have worse prognosis.<sup>6</sup> Blood vessels in LGGs are usually less abnormal, but a proportion of IDH-wildtype LGGs show early changes in gene expression that are similar to those found in GBM, although not as pronounced.<sup>7</sup> The mechanisms underlying dysfunctional vessels and their role in therapy resistance are still largely unknown.

Several genes are differentially expressed in human glioma vessels as compared to normal brain vessels, including epidermal growth factor, latrophilin, and seven transmembrane domain-containing protein 1 (ELTD1).<sup>8,9</sup> ELTD1 is an orphan member of the adhesion G-protein-coupled receptor (GPCR) family that is highly expressed in the microvasculature.<sup>10,11</sup> ELTD1 is frequently upregulated in tumor vessels and was included in a 20-gene tumor angiogenesis signature identified in a meta-analysis to define proteins involved in the transcriptional control of tumor angiogenesis in human cancer.<sup>12</sup> ELTD1 has been suggested as a biomarker for high-grade gliomas, and anti-ELTD1 antibodies reduced glioma growth and decreased microvessel density in orthotopic glioma models.<sup>13–15</sup> However, the role of ELTD1 in regulating endothelial phenotype and its impact on the glioma microenvironment have not been investigated.

In this report, we evaluated the role of ELTD1 in GBM by assessing its expression patterns, identifying co-expressed genes in patient tumors, and analyzing the impact of ELTD1 deletion in orthotopic, syngeneic glioma models.

ELTD1 expression increased with tumor malignancy in human gliomas and correlated with expression of genes associated with abnormal GBM vessels. ELTD1 deletion did not affect tumour growth but resulted in improved vessel function, as indicated by reduced hypoxia and fibrinogen leakage as well as enhanced lectin perfusion. Transcriptional profiling indicated that the tumor endothelium was less proliferative in ELTD1<sup>-/-</sup> mice, whereas the inflammatory response was increased. Consistent with this, infiltration of CD8<sup>+</sup> T cells was enhanced after PD-1 (programmed cell death protein 1) blockade immunotherapy in ELTD1<sup>-/-</sup> mice, and median survival was prolonged. Our data indicate that ELTD1 deletion does not perturb angiogenesis, but instead normalizes tumor vessels and improves the efficacy of cancer immunotherapy.

## Materials and Methods

### Tissue Microarray Analysis

ELTD1 expression was analyzed in tissue microarrays (TMAs) containing duplicate tissue cores (1 mm in diameter) of 113 biopsies representing 14 IDH-wildtype diffuse astrocytomas (AII, IDHwt), 37 IDH-mutated, 1p/19q non-codeleted astrocytomas (AII, IDHmut), 12 IDH-wildtype anaplastic astrocytomas (AIII, IDHwt), 43 GBM (IDHwt), and 7 control brains. Immunohistochemistry was performed as described<sup>8</sup> using anti-ELTD1 (HPA025229, Sigma-Aldrich) and 3,3'-diaminobenzidine (DAB) as substrate. Slides were counterstained with hematoxylin, mounted using a Leica Autostainer XL (Leica Microsystems), and scanned using a ScanScope XT system (Aperio Technologies, Vista, CA) at ×20 magnification. ELTD1 vascular staining was scored

from 0 to 3 (0 = no staining, 1 = low, 2 = medium, 3 = high intensity) by 2 researchers blindly and individually. Results were plotted according to the WHO 2016 glioma classification.<sup>17</sup> Astrocytic gliomas (1p/19q non-codeleted) were included in a survival analysis. Detailed patient information is available in [Supplementary Table 1](#). Human tissue was obtained in a manner compliant with the Declaration of Helsinki. The Ethics Review Board in Uppsala approved the use of human samples and the use of TMAs was granted by Uppsala County's ethical committee (Dnr Ups 02-330, Ups 06-084, Dnr Ki 02-254, Ups 03-412/2003-10-02, Dnr 2010/291).

### Mice

C57BL/6 mice with a global knockout of ELTD1 (ELTD1<sup>-/-</sup>) were generated as described in the [Supplementary Materials and Methods](#). Heterozygotes were bred in-house and wildtype littermates were used as controls. All animal work was performed according to the guidelines for animal experimentation and welfare provided by Uppsala University and approved by the Uppsala County regional ethics committee (Dnr C26/15, Dnr C1/14, Dnr 5.8.18-19429-2019).

### Cell Culture

GL261 (gift from Dr. Safrany, NRIRR, Budapest, Hungary) and CT-2A (gift from Dr. Vähä-Koskela, Ottawa Hospital Research Institute) glioma cells were cultured in Dulbecco's modified Eagle medium (Life Technologies) supplemented with 10% fetal bovine serum (Sigma-Aldrich) at 37°C and 5% CO<sub>2</sub>/95% air in a humidified chamber.

### Tumor Studies

GL261 or CT-2A glioma cells were orthotopically injected in the brain of ELTD1<sup>-/-</sup> and wildtype mice as described in the [Supplementary Materials and Methods](#). For survival studies, mice were sacrificed when they lost more than 10% body weight or exhibited symptoms of a brain tumor. For the anti-PD-1 study, 200 µg of anti-mouse PD-1 (RMP1-14, Cat. # BE0146, InVivoMab, BioXcell) or rat-isotype IgG2a control (2A3, #BE089, InVivoMab, BioXcell) were administered intravenously every 3 days, starting on day 10 after tumor injection up to a total of 4 administrations.

### Vessel Perfusion and Tumor Hypoxia Studies

Tumor vessel perfusion was assessed by injecting 100 µg of biotinylated *Lycopersicon esculentum* (tomato) lectin (Vector Laboratories) in the orbital plexus at endpoint. Lectin was allowed to circulate for 5 minutes, after which mice were intracardially perfused with PBS followed by 4% paraformaldehyde. Tumor hypoxia was assessed by Hypoxyprobe-Red549 Kit (HP7-x, Hypoxyprobe Inc, Burlington, MA). Briefly, hypoxyprobe was injected intraperitoneally 1 hour prior to sacrificing the mice, and hypoxia was visualized by a detection antibody staining on tumor sections.

### Immunofluorescence Staining

Cryosections (10 µm) and vibratome sections (80 µm) from mouse brain tumors were stained for CD31, fibrinogen, desmin, Lef1, CD8, CD3, and CD45 as described in the [Supplementary Materials and Methods](#). Samples were analyzed under the confocal microscope (Leica SP8) or fluorescent microscope (Leica DMI8). Staining intensities and tumor areas were quantified by ImageJ software.

### Translating Ribosome Affinity Purification (TRAP) Methodology

C57BL/6 mice expressing a fusion eGFP-L10a ribosomal protein under control of the endothelial-specific promoter VE-cadherin (VEcadTRAP mice)<sup>16</sup> were crossed with ELTD1<sup>-/-</sup> mice. Mice were intracranially injected with GL261 cells, brains were harvested at day 23 after tumor injection, and tumors were dissected under a stereological microscope. Brains from healthy mice were used as controls. Endothelial ribosomes were purified and mRNA was extracted as described.<sup>18,19</sup> Briefly, eGFP-tagged polysomes were isolated using anti-GFP-bound Dynabeads (Qiagen), endothelial cell mRNA was extracted using Trizol and purified by RNeasyMicro kit (Qiagen).

### RNA-Seq Library Preparation and Sequencing

Ribosomal RNA was removed using the RiboGone kit (Clontech Laboratories). The RNA quality was assessed by Agilent 2100 bioanalyzer. Samples with RIN value >7 were selected for cDNA synthesis and purification. Tumor samples from 3 wildtype and 3 ELTD1<sup>-/-</sup> mice were selected for library preparation using SMARTer<sup>®</sup> Stranded RNA-Seq Kit (Clontech Laboratories) and sequenced on HiSeq2500.

### RNA Sequencing Data Analysis

The sequence reads were aligned to the Ensembl mouse gene assembly (version: GRCh38) and expression quantification was performed using TopHat2 software (version 2.0.4).<sup>20</sup> To identify differentially expressed genes, statistical tests were performed using the Cufflinks tool (version 2.2.1). Genes with multiple test corrected  $P < .05$  were considered as significantly differentially expressed. Computations were performed on resources provided by Swedish National Infrastructure for Computing through Uppsala Multidisciplinary Center for Advanced Computational Science (UPPMAX) under Project SNIC 2017/7-240. The RNA sequencing data were submitted to the NCBI GEO database under the series accession number GSE152635. Gene set enrichment analysis (GSEA) was performed using the molecular signatures database hallmark gene set collection by software GSEA\_4.0.3. Gene ontology (GO) term enrichment analysis was performed using the online gene annotation and analysis resource Metascape.<sup>21</sup>

### Survival Analysis, Gene Correlation Analysis, and Statistical Analysis

Correlations between ELTD1 expression and patient survival were performed using the CGGA<sup>22</sup> and TCGA glioma

datasets, downloaded from the Gliovis data portal (<http://gliovis.bioinfo.cnio.es>) using a median cutoff. The *P* value was determined using the log-rank test, and *P* < .05 was considered statistically significant.

REMBRANDT,<sup>23</sup> Bao, Reifenger, LeeY, Murat, Oh, Frejje, Philips, and Walsh datasets were downloaded and included for gene correlation analysis. Genes that correlated with ELTD1 expression with  $|r| > 0.3$  were selected for comparison between datasets.

The IVY Gap database (<https://glioblastoma.alleninstitute.org/>) was used to analyze ELTD1 expression in different anatomical regions of the tumor. Statistical analysis was performed using unpaired Student's *t* test or ordinary 1-way ANOVA in GraphPad Prism 6.0 software (GraphPad Inc., La Jolla, CA). For mouse survival studies, statistical analysis was performed using the log-rank test or Gehan-Breslow-Wilcoxon test. A *P* value < .05 was considered statistically significant.

## Results

### ELTD1 Expression in Glioma Vessels Correlates With Tumor Malignancy and Poor Patient Survival

We previously demonstrated that ELTD1 was upregulated in GBM vessels as compared to normal brain vessels.<sup>8</sup> To extend the analysis to a larger cohort and determine if the level of ELTD1 in the vasculature was associated with tumor malignancy, we analyzed ELTD1 protein expression in human TMAs. ELTD1 was detected in control brain and tumor tissue and was specifically expressed in the vasculature. We assessed its expression based on the intensity of the staining from 0 to 3 (representing no, low, medium, and high intensity) (Figure 1A). ELTD1 expression in the vasculature positively correlated with glioma malignancy, with the highest levels observed in the most malignant tumors (IDHwt AIII and GBM) whereas its expression in IDHmut AII and IDHwt AII tumors was similar to control brain (Figure 1B). Consistent with this, high expression of ELTD1 in tumor blood vessels was associated with poor survival of astrocytoma patients (Figure 1C). To evaluate the correlation between ELTD1 expression, tumor malignancy, and survival, we analyzed data from the CGGA and TCGA databases. ELTD1 gene expression positively correlated with tumor malignancy with the highest expression found in the GBM group (Figure 1D, Supplementary Figure S1A). High ELTD1 expression correlated with poor survival of patients with astrocytoma in both the CGGA and TCGA database (Figure 1E, Supplementary Figure S1B). To extend these data, we analyzed patient survival in specific glioma groups separately. ELTD1 expression significantly correlated with survival both in the IDHmut gliomas and in the more aggressive IDHwt tumors (AIII-GBM) in the CGGA dataset (Figure 1F and G), while only a trend was observed when analyzing survival of GBM patients in the TCGA dataset (Supplementary Figure S1C). In summary, ELTD1 expression is associated with a higher malignancy grade and poor prognosis for patients with astrocytoma.

### ELTD1 Deletion Does Not Disrupt Vascular Development in Mice

To determine the role of ELTD1 in vascular development, ELTD1-deficient mice were generated. ELTD1 mRNA expression was detected in highly vascularized organs such as heart, brain, kidney, lung, and retina (Supplementary Figure S2A). The ELTD1 gene was disrupted by the replacement of coding exon 3 to 13 with TMLacZ lox-Ub1-EM7-Neo-lox cassette (Supplementary Figure S2B). Successful deletion of ELTD1 was confirmed by genotyping, qPCR, and western blot (Supplementary Figure S2C–E). ELTD1<sup>-/-</sup> mice were viable and born at normal Mendelian ratios. To assess the potential role of ELTD1 in vascular development, we analyzed the vasculature in the retina at postnatal day 6. No difference was observed in the vascular area (Supplementary Figure S2F) or sprouting front (Supplementary Figure S2G) when comparing wildtype and ELTD1<sup>-/-</sup> mice. Similarly, the tissue morphology of liver, kidney, and lung was normal in ELTD1<sup>-/-</sup> mice, and the vasculature was indistinguishable from wildtype mice (Supplementary Figure S2H and I). Consistent with ELTD1 being dispensable for vessel formation, siRNA-mediated knockdown of ELTD1 (Supplementary Figure S3A and B) in human dermal microvascular endothelial cells (HDMECs) did not affect proliferation (Supplementary Figure S3C), migration (Supplementary Figure S3D), or formation of tubular structures (Supplementary Figure S3E and F). Thus, our data indicate that ELTD1 expression is dispensable for angiogenesis and vascular development.

### ELTD1 Deletion Does Not Affect Progression of Orthotopic Murine Glioma

To investigate if the host expression of ELTD1 affects tumor growth, we employed the GL261 and CT-2A syngeneic, orthotopic glioma models. Glioma cells were transplanted intracranially in wildtype and ELTD1<sup>-/-</sup> mice, and allowed to grow for 23 days before the mice were sacrificed, brains were collected and tumor area was measured in tissue sections. The tumor sizes of orthotopic GL261 and CT-2A gliomas were similar in ELTD1<sup>-/-</sup> mice and wildtype mice (Figure 2A and B). In experiments where mice instead were sacrificed when they showed symptoms of a brain tumor, ELTD1 deletion did not affect mouse survival in either glioma model (Figure 2C and D). These data demonstrate that ELTD1 deletion does not affect tumor progression in orthotopic glioma models.

### ELTD1 Deletion Is Associated With Enhanced Vessel Function in Murine Glioma

To determine if ELTD1 regulates vessel function, we analyzed GL261 tumor vasculature in wildtype and ELTD1<sup>-/-</sup> mice. Vascular density was unchanged in ELTD1<sup>-/-</sup> mice (Figure 3A and B), but an improvement in tumor vessel functionality was observed as compared to wildtype mice. Indeed, lectin perfusion of GL261-bearing mice revealed a significantly increased vessel perfusion in ELTD1<sup>-/-</sup> mice (Figure 3A and C). Vascular leakage was assessed by the



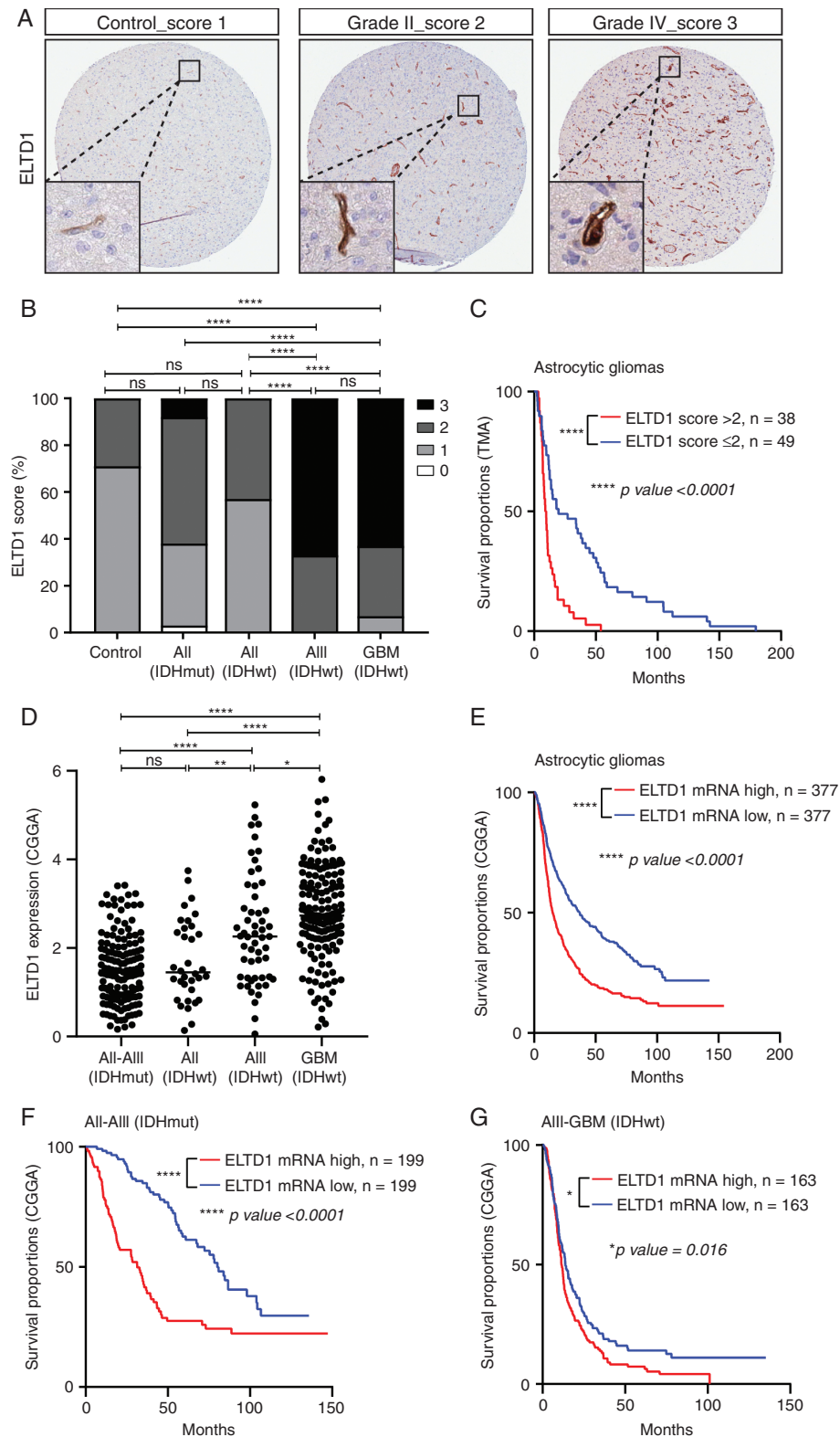


**Fig. 1** ELTD1 expression in glioma vessels correlates with tumor malignancy and poor patient survival. (A) Immunohistochemistry staining of ELTD1 in human glioma TMAs. ELTD1 intensity in tumor vessels was scored on a scale from 0 to 3 (indicating no, low, medium, or high intensity). (B) Semi-quantitative scoring of ELTD1 in non-tumor control brains (n = 7), IDH-mutated astrocytoma (All, IDHmut, n = 37), IDH-wildtype diffuse astrocytoma (All, IDHwt, n = 14), and high-grade glioma IDH-wildtype anaplastic astrocytoma (All, IDHwt, n = 12) and IDH-wildtype glioblastoma (GBM, IDHwt, n = 43). Kruskal-Wallis test with Dunn's post-test. (C) Survival analysis of all astrocytic glioma patients with high vascular ELTD1

presence of fibrinogen, which leaks into the brain when the blood-brain barrier is disrupted. A reduction in fibrinogen was observed in gliomas from ELTD1<sup>-/-</sup> mice as compared to the wildtype group, indicative of reduced vascular permeability (Figure 3D and E). Consistent with better tumor vessel functionality in ELTD1<sup>-/-</sup> mice, tumor hypoxia was reduced (Figure 3F and G). However, the extent of pericyte coverage in the vessels, as determined by desmin staining, was not altered (Figure 3H and I, Supplementary Figure S4E and F), suggesting that ELTD1 does not affect interactions between pericytes and endothelial cells. The Wnt signaling pathway is important for maintaining vascular barrier function in the brain and is upregulated during the establishment of the blood-brain barrier. To investigate whether the normalization of tumor vasculature in ELTD1<sup>-/-</sup> mice was associated with enhanced Wnt signaling, we analyzed Lef1, a key transcription factor of the Wnt/ $\beta$ -catenin pathway. Lef1 was preferentially detected around the tumor border (Figure 3J), and the number of Lef1 positive vessels was increased in ELTD1<sup>-/-</sup> mice (Figure 3K).

An improvement of tumor vessel function was also observed in CT-2A tumors in ELTD1<sup>-/-</sup> mice. Vascular density and perfusion were unchanged, related to a comparatively high proportion of perfused vessels in this model, but fibrinogen leakage was strongly reduced and the proportion of Lef1<sup>+</sup> vessels was increased in ELTD1<sup>-/-</sup> mice as compared to wildtype (Supplementary Figure S4A–H).

Thus, our data show that tumor vascular dysfunction was reduced in ELTD1-deficient mice, while expression of Lef1 was enhanced, indicating that loss of ELTD1 normalizes tumor vessels and improves the blood-brain barrier function.

### ELTD1 Expression Correlates With Genes Associated With Vascular Abnormalities in Human Glioma

To analyze the expression of ELTD1 in different anatomical regions of the tumor, we employed the IVY Gap database (<https://glioblastoma.alleninstitute.org/>), which includes RNA sequencing data for the leading edge, infiltrating tumor, cellular tumor, microvascular proliferation, and pseudopalisading cells surrounding necrosis. Consistent with a predominant expression in tumor endothelial cells, ELTD1 was highly enriched in microvascular proliferation in all available GBM samples (Supplementary Figure S5).

ELTD1 deletion normalizes the tumor vasculature in murine glioma. To determine if ELTD1 expression is associated with vascular abnormalities in human glioma, we downloaded 12 datasets from the GliOVis portal which contain gene expression data from tumors surgically removed from patients with GBM, and analyzed genes that are correlated with ELTD1 using the threshold  $|r| > 0.3$ ,  $P < .05$ . Genes that were co-expressed with ELTD1 in at least 6 datasets, and

with  $|r| > 0.7$  in the CGGA database are displayed in Figure 4A. ELTD1 expression correlates with vascular marker genes including CD34, CDH5, and PECAM1, consistent with its expression in endothelial cells. We have analyzed genes preferentially expressed in vessels from glioma and control brains, and identified those significantly enriched in GBM vessels.<sup>8</sup> By filtering the list of correlated genes to only include those preferentially expressed in vessels, we found 39 vascular genes that were co-expressed with ELTD1. Amongst these, 15 genes were previously identified as upregulated in abnormal GBM vessels as compared to normal brain vessels, including ANGPT2, CD93, and FN1 (Figure 4B).<sup>8,24–26</sup> This demonstrates that ELTD1 expression is associated with a gene expression signature previously coupled to vascular abnormalities in human GBM.

### ELTD1 Deletion Results in Upregulation of Genes Associated With Inflammatory Response

To understand how ELTD1 deficiency affects the tumor microenvironment, we analyzed tumor endothelial transcripts by RNA sequencing. ELTD1<sup>-/-</sup> and wildtype mice were crossed with mice expressing an eGFP-tagged-L10a ribosomal protein under control of the VE-cadherin promoter.<sup>16</sup> Endothelial specific mRNA was isolated from GL261 tumors by isolation of eGFP-tagged ribosomes and prepared for RNA sequencing analysis. Functional gene networks influenced by ELTD1 deletion were identified using GSEA and GO term analysis of the tumor endothelial transcripts. The GSEA analysis revealed a downregulation of Myc and E2F pathways in tumor endothelial cells from ELTD1<sup>-/-</sup> mice (Figure 5A), suggesting a more quiescent tumor endothelium in ELTD1<sup>-/-</sup> mice. Moreover, the GSEA analysis revealed an enrichment of pathways associated with inflammatory response and interferon alpha and gamma responses in ELTD1<sup>-/-</sup> mice, suggesting that ELTD1 deletion may enhance the immune response in the microenvironment (Figure 5B and C). To validate the expression of genes associated with inflammatory response, we stained for endothelin 1 (EDN1) and ICAM1 in the GL261 tumors. Both EDN1 and ICAM1 expression were significantly increased in tumor vessels in ELTD1<sup>-/-</sup> mice as compared to those in wildtype mice (Figure 5D and E). A total of 168 genes were differentially expressed in ELTD1<sup>-/-</sup> tumor endothelial cells as compared to wildtype (threshold  $q$  value  $< 0.1$ ) (Supplementary Table 2). GO term enrichment analysis of the differentially expressed genes revealed an enrichment of genes associated with antigen processing and presentation (Supplementary Figure S6A). These included the MHC class I molecules H2-D1 and H2-Ab1, responsible for displaying antigens for T cells, and the chemokine CXCL12 which is chemotactic for lymphocytes (Supplementary Figure S6B), suggesting that T-cell responses may be enhanced in gliomas in ELTD1<sup>-/-</sup> mice.

expression (score  $> 2$ ,  $n = 38$ ) and low ELTD1 vascular expression (score  $\leq 2$ ,  $n = 49$ ). (D) ELTD1 mRNA expression from the CGGA database. (E) Survival analysis of astrocytic glioma patients from the CGGA database. (F) Survival analysis of IDHmut AII–AIII patients and (G) IDHwt AIII–GBM patients from the CGGA database. Statistical analysis of survival rates was assessed by univariate model (log-rank test). \*\*\*\* $P < .0001$ , \*\* $P < .01$ , \* $P < .05$ . Abbreviations: GBM, Glioblastoma; IDH, isocitrate dehydrogenase; ns, not significant; TMA, tissue microarray.

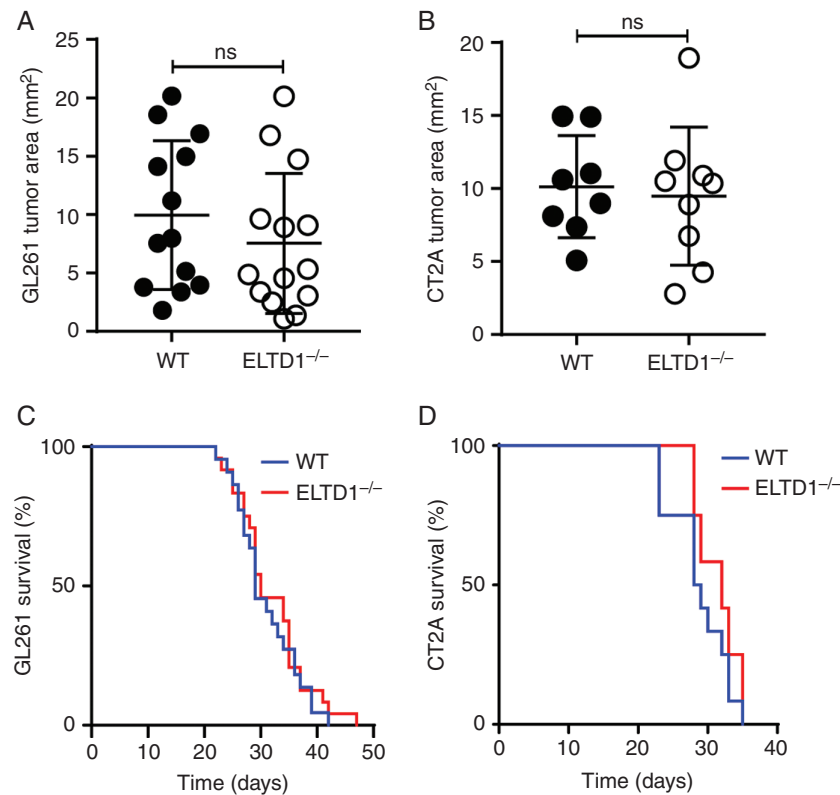


**Fig. 2** ELTD1 deletion does not affect glioma growth or survival in murine models. (A) GL261 and (B) CT-2A tumor size on day 23 after inoculation in wildtype (WT) and ELTD1<sup>-/-</sup> mice. Values represent tumor area identified by nuclear staining. Survival analysis of (C) GL261 and (D) CT-2A glioma injected mice. ns = not significant. Statistical analysis of survival rates was assessed by univariate model (log-rank test).

Taken together, gene expression profiling of tumor endothelial cells indicates a less proliferative tumor endothelium and enhanced inflammatory responses in gliomas in ELTD1<sup>-/-</sup> mice.

### ELTD1 Deletion Improves the Response to PD-1 Blockade Immunotherapy

Cancer immunotherapy can be improved by increased vessel function and enhanced inflammatory response of tumor endothelial cells,<sup>4</sup> suggesting that the efficacy of checkpoint blockade may be augmented in ELTD1<sup>-/-</sup> mice. To evaluate this hypothesis, we investigated the response to PD-1 checkpoint blockade in wildtype and ELTD1<sup>-/-</sup> GL261 tumor-bearing mice by treating with anti-PD-1 or isotype IgG. The therapeutic PD-1 antibody was detected both inside and around the tumor (Supplementary Figure S7). Anti-PD-1 treatment significantly improved survival in both wildtype and ELTD1<sup>-/-</sup> mice. Moreover, compared to 35 days in the wildtype anti-PD-1 group, median survival after anti-PD-1 therapy was further prolonged to 47 days in ELTD1<sup>-/-</sup> mice. The isotype control groups had median survival of 30 and 33 days in the ELTD1<sup>-/-</sup> and wildtype groups respectively (Figure 6A). The total number of immune cells, detected by CD45 staining, was similar in all groups (Supplementary Figure S8). However, CD3<sup>+</sup> total T cells and

CD8<sup>+</sup> cytotoxic T cells were most abundant in the anti-PD-1-treated ELTD1<sup>-/-</sup> group, and were significantly increased as compared to the anti-PD-1-treated wildtype group (Figure 6B and C). An increased infiltration of CD8<sup>+</sup> T cells was also noted in CT-2A tumors in ELTD1<sup>-/-</sup> mice (Supplementary Figure S9). These results indicate that T-cell recruitment is improved in gliomas in ELTD1<sup>-/-</sup> mice, of benefit for PD-1 blockade immunotherapy.

## Discussion

ELTD1 has been suggested as a potential target for anti-angiogenic therapy.<sup>8,12,27</sup> We demonstrate that ELTD1 is dispensable for tumor angiogenesis, but that it contributes to the development of vascular abnormalities in glioma. Deletion of ELTD1 normalized vessels, improved inflammatory activation of tumor endothelial cells, and enhanced T-cell recruitment, indicating a benefit of targeting ELTD1 in combination with cancer immunotherapy.

ELTD1 expression was strongly associated with poor patient survival in both IDHmut AII-AIII tumors and IDHwt AIII-GBM in the CGGA dataset. However, only a nonsignificant trend was observed when analyzing GBM separately in the TCGA dataset, suggesting that the prognostic impact of ELTD1 is more pronounced in tumors where there is a

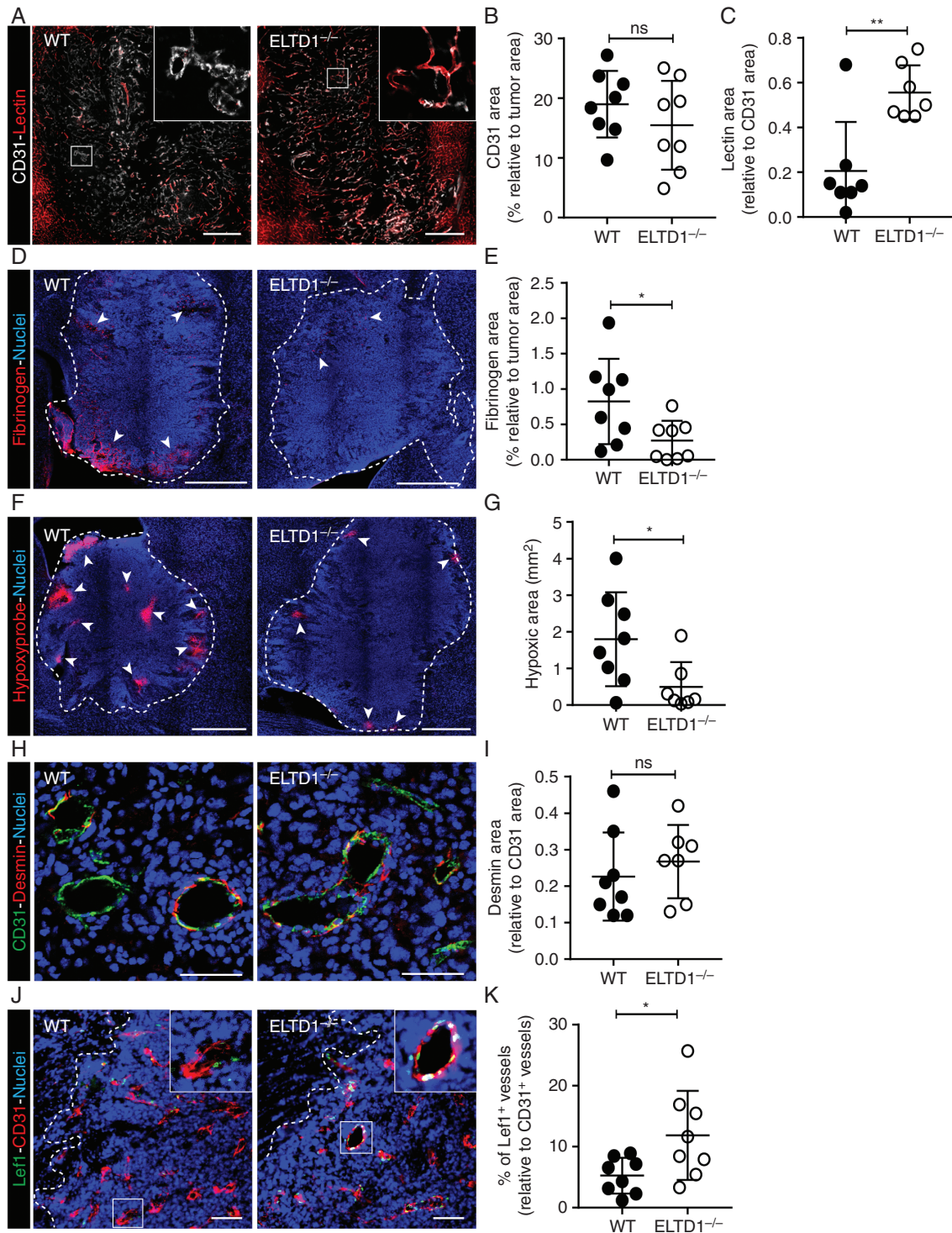


**Fig. 3** ELTD1 deletion is associated with enhanced vessel function in GL261 tumors. (A) Representative images of GL261 tumor vasculature in wildtype and ELTD1<sup>-/-</sup> mice. Vessels are visualized by CD31 (white) and perfused vessels by lectin (red). Scale bar: 500 μm. (B) Quantification of CD31<sup>+</sup> vessels relative to tumor area. (C) Quantification of lectin perfused vessels normalized by CD31<sup>+</sup> area. (D) Immunofluorescent images of fibrinogen leakage (red). Dotted line indicates GL261 tumor border and arrowheads fibrinogen extravasation. Scale bar: 500 μm. (E) Quantification of intratumoral fibrinogen<sup>+</sup> area. (F) Tumor hypoxic area detected by hypoxyprobe (red). Dotted line indicates tumor border and arrowheads the hypoxic area. Scale bar: 500 μm. (G) Tumor hypoxia quantification. (H) Pericyte coverage of tumor vessels visualized by desmin (red) and CD31 (green). Scale bar: 50 μm. (I) Quantification of desmin<sup>+</sup> pericytes relative to CD31<sup>+</sup> area. (J) Immunofluorescent images of Lef1 (green) and CD31 (red). Dotted line indicates tumor border. Scale bar: 50 μm. (K) Quantification of Lef1 relative to CD31<sup>+</sup> vessels. \*\**P* < .01, \**P* < .05, ns = not significant, 2-tailed *t* test.



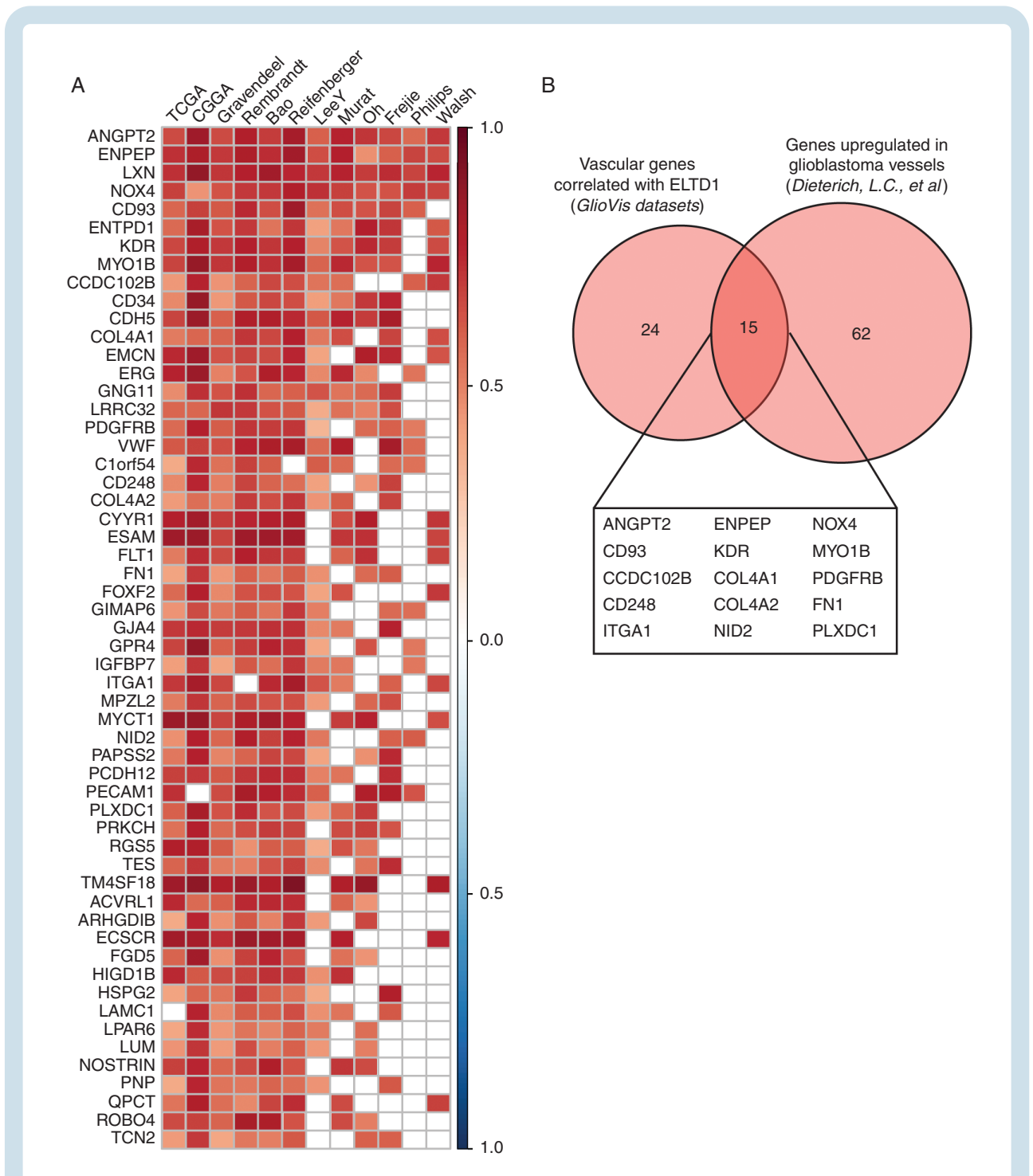


**Fig. 4** ELTD1 expression in human glioma correlates with genes associated with vascular abnormalities. (A) Heat map depicting genes significantly correlated with ELTD1 in at least 6 out of 12 datasets representing glioblastoma patients downloaded from the GlioVis portal ( $|r| > 0.7$  in the CGGA dataset,  $|r| > 0.3$  and  $P < .05$  were considered as cutoff for correlation). The color scale represents the  $r$  value in each dataset. (B) Venn diagram showing the overlap ( $n = 15$ ) of genes co-expressed with ELTD1 in the GlioVis datasets ( $n = 39$ ) and genes previously identified as upregulated in glioblastoma vessels ( $n = 77$ ).<sup>8</sup>

higher variance in the extent of vascular abnormality.<sup>7</sup> This discrepancy may also be due to differences in sample acquisition. The CGGA database contains samples that were more recently obtained, and has a higher number of

samples from deceased patients ( $n = 553$ ) than the TCGA database ( $n = 221$ ). Glioma treatment has been improved and standardized over the years, and the CGGA data may be more consistent with today's therapeutic regimens. In

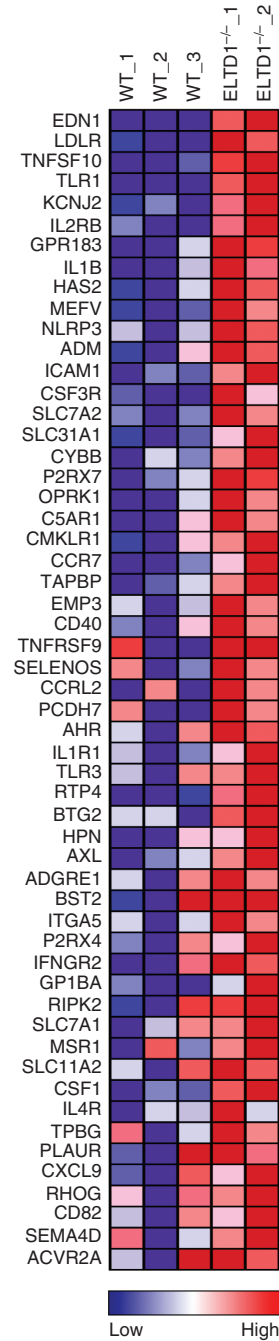
**A** Down-regulated gene sets in ELTD1<sup>-/-</sup> tumor ECs

RANK	GENE SET	NES	FDR q-val
1	MYC_TARGETS_V2	-1.661	0.027
2	MYC_TARGETS_V1	-1.594	0.021
3	E2F_TARGETS	-1.468	0.039
4	G2M_CHECKPOINT	-1.405	0.049

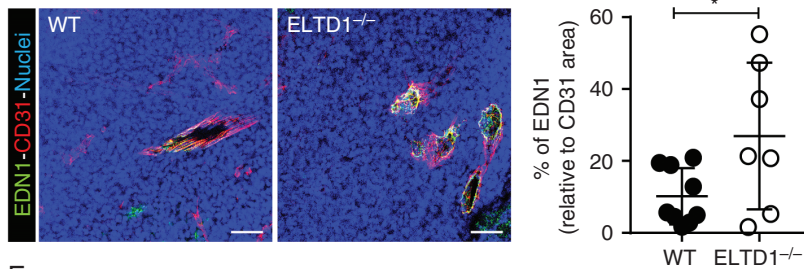
**B** Up-regulated gene sets in ELTD1<sup>-/-</sup> tumor ECs

RANK	GENE SET	NES	FDR q-val
1	EPITHELIAL_MESENCHYMAL_TRANSITION	2.305	<0.001
→ 2	INFLAMMATORY_RESPONSE	2.104	<0.001
3	CHOLESTEROL_HOMEOSTASIS	2.096	<0.001
→ 4	INTERFERON_GAMMA_RESPONSE	2.085	<0.001
5	MTORC1_SIGNALING	2.055	<0.001
6	HYPOXIA	2.023	<0.001
7	IL6_JAK_STAT3_SIGNALING	1.996	<0.001
8	ALLOGRAFT_REJECTION	1.943	<0.001
→ 9	INTERFERON_ALPHA_RESPONSE	1.889	<0.001
10	COAGULATION	1.809	0.001
11	IL2_STAT5_SIGNALING	1.715	0.004
12	COMPLEMENT	1.698	0.004
13	GLYCOLYSIS	1.689	0.005
14	UV_RESPONSE_DN	1.670	0.005
15	NOTCH_SIGNALING	1.595	0.011
16	KRAS_SIGNALING_UP	1.587	0.012
17	ANDROGEN_RESPONSE	1.584	0.011
18	APOPTOSIS	1.500	0.026
19	BILE_ACID_METABOLISM	1.487	0.028
20	TNFA_SIGNALING_VIA_NFKB	1.434	0.046

**C** Upregulated hallmark genes of inflammatory response



**D**



**E**

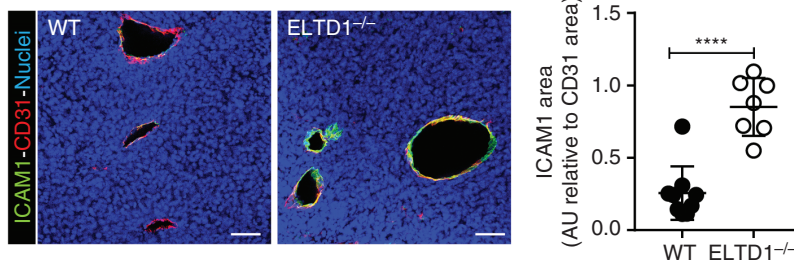


**Fig. 5** ELTD1 deletion results in the expression of genes associated with enhanced inflammatory response. GSEA analysis of downregulated (A) and upregulated (B) gene sets from RNA sequencing performed in GL261 tumor endothelial cells isolated from wildtype (n = 3) and ELTD1<sup>-/-</sup> (n = 3) mice (threshold for GSEA FDR <0.05). Arrows in B indicate pathways related to immune response. (C) Hallmark genes of inflammatory response upregulated in ELTD1<sup>-/-</sup> tumor endothelial cells. Two tumor samples were pooled together for RNA sequencing in the ELTD1<sup>-/-</sup> group due to a low amount of material. (D) Representative immunofluorescence image of endothelin 1 (EDN1, green) and CD31 (red) in GL261 tumors from ELTD1<sup>-/-</sup> and WT mice. Quantification represents EDN1 levels relative to CD31<sup>+</sup> area. (E) Representative immunofluorescence image of ICAM1 (green) and CD31 (red) in GL261 tumors from ELTD1<sup>-/-</sup> and WT mice. Quantification represents ICAM1<sup>+</sup> area relative to CD31<sup>+</sup> area. \*\*\*\*P < .0001, \*P < .05, 2-tailed t test. Abbreviations: FDR, false discovery rate; GSEA, gene set enrichment analysis; WT, wildtype.

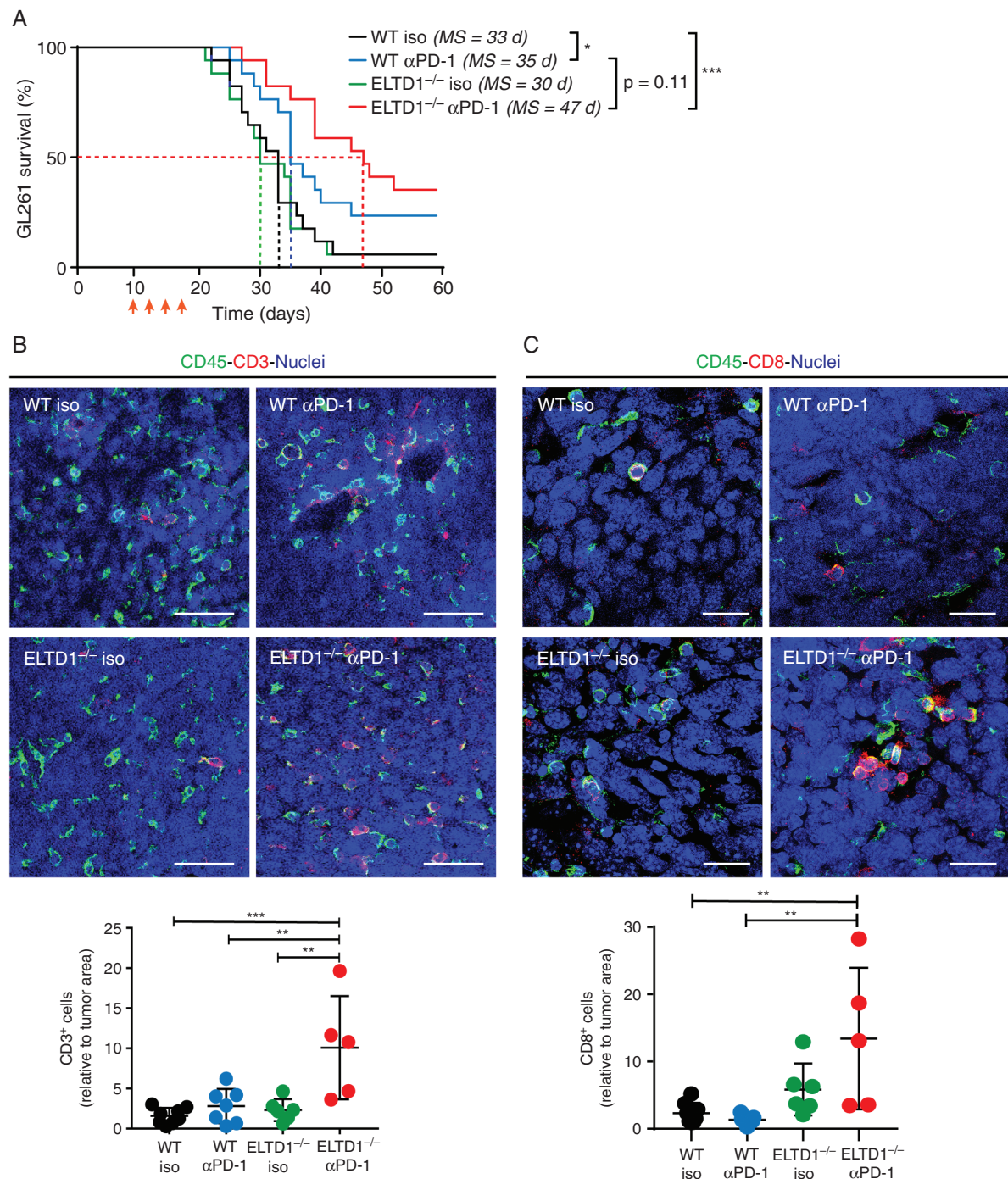


**Fig. 6** ELTD1 deletion prolongs survival of glioma-bearing mice after PD-1 blockade. (A) Survival of GL261 tumor-bearing mice treated with anti-PD-1 ( $\alpha$ PD-1) or isotype IgG (iso) in wildtype mice and ELTD1<sup>-/-</sup> mice (n = 17 in each group). Arrows indicate days of administration of anti-PD-1 or isotype IgG control (days 10, 13, 16, and 19 after injection). MS: median survival. Statistical analysis of survival rates was assessed by univariate model (Gehan-Breslow-Wilcoxon test, \* $P < .05$ , \*\*\* $P < .001$ ). (B) Immunofluorescent images of CD45<sup>+</sup> cells (green) and CD3<sup>+</sup> cells (red) in GL261 tumors from wildtype (WT) and ELTD1<sup>-/-</sup> mice treated with anti-PD-1 or isotype IgG. Scale bar: 50  $\mu$ m. Quantification represents the number of CD3<sup>+</sup> cells relative to tumor area. (C) Immunofluorescent images of infiltrated CD45<sup>+</sup> cells (green) and CD8<sup>+</sup> cells (red) in GL261 tumors from wildtype and ELTD1<sup>-/-</sup> mice treated with anti-PD-1 or isotype IgG. Scale bar: 25  $\mu$ m. Quantification represents the number of CD8<sup>+</sup> cells relative to tumor area. \* $P < .05$ , \*\* $P < .01$ , \*\*\* $P < .001$ ; Tukey's multiple comparison test. Abbreviation: PD-1, programmed cell death protein 1.



GBM, there are extensive vascular abnormalities, and the effect that was observed in the CGGA dataset could be due to enhanced transport of drugs in tumors with lower levels of ELTD1.

Vascular normalization achieved by anti-angiogenic drugs can improve the response to cancer immunotherapy.<sup>16</sup> However, tyrosine kinase inhibitors or antibodies targeting the vascular endothelial growth factor (VEGF) pathway only improve vessel function in a subset of GBM patients.<sup>28,29</sup> These therapies rely on restoring the level of VEGF signaling in normal vessels, which narrows the therapeutic window.<sup>7</sup> Targeting of ELTD1 may be preferable to inhibiting VEGF pathways and give less side effects. While mice deficient in ELTD1 are healthy and lack vascular defects, the VEGF pathway is important for vascular homeostasis and endothelial cell survival.<sup>30</sup> ELTD1-targeting antibodies have been demonstrated to reduce tumor growth in glioma models.<sup>13-15</sup> However, the underlying mechanisms are unclear since these antibodies also bound to the glioma cells rather than specifically to the vessels, suggesting that antibody-dependent cellular cytotoxicity may have also contributed. Notably, vascular normalization may not always be of benefit as decreased vascular perfusion was associated with reduced transport of temozolomide in patients with recurrent GBM.<sup>29</sup> Treatment efficacy may instead be enhanced by a more specific breakdown of the blood-brain barrier, similar to what was observed in WNT medulloblastomas.<sup>31</sup> The connection between tumor vascular phenotypes and specific drug responses is an important area for further investigation.

The transcriptional analysis revealed distinct tumor endothelial gene expression signature in gliomas in ELTD1<sup>-/-</sup> mice, indicative of an altered vascular phenotype. Although bioinformatic analysis of gene expression signatures can provide insights into cellular biology, there are several drawbacks. For instance, among the genes that are included in the GSEA hypoxia gene set, SLC2A1 (Glut1) is a glucose transporter constitutively expressed in cerebral endothelial cells,<sup>32</sup> and ADM (adrenomedullin) is an important regulator of blood-brain barrier function.<sup>33</sup> Thus, the fact that SLC2A1 and ADM are increased in ELTD1<sup>-/-</sup> tumor endothelial cells is not indicative of increased hypoxia but reflects normal gene expression of brain endothelial cells. Similarly, we did not observe downregulation of endothelial genes, indicating that the observed epithelial-mesenchymal transition signature is not indicative of endothelial-mesenchymal transition. The Myc pathway was downregulated in tumor endothelial cells in ELTD1<sup>-/-</sup> mice, consistent with less proliferative tumor endothelial cells. The FOXO1-Myc transcriptional network regulates metabolic activity during endothelial proliferation<sup>34</sup> and ELTD1 can affect endothelial metabolism.<sup>35</sup> Our finding that interferon (IFN) response genes were upregulated in tumor endothelial cells in ELTD1<sup>-/-</sup> mice is consistent with the emerging role of vascular normalization in improving T-cell infiltration and enhancing the response to immunotherapy.<sup>4</sup> Activated T cells secrete IFN, suggesting that the increased transcription of IFN response genes may be associated with enhanced

recruitment and/or activation of T cells. Indeed, the T-cell-attracting chemokines CXCL9 and CXCL12 were upregulated in tumor endothelial cells in ELTD1<sup>-/-</sup> mice. The observed upregulation of MHC class I molecules may indicate an antigen-presenting function of tumor endothelial cells in ELTD1<sup>-/-</sup> mice and/or enhanced chemotaxis of T cells. Endothelial cells have been implicated as antigen-presenting cells in human diseases,<sup>36</sup> and T cells that recognize antigens on the apical surface of endothelial cells are induced to transmigrate through the endothelial barrier.<sup>37</sup> In agreement with an enhanced inflammatory activation of tumor endothelial cells in ELTD1<sup>-/-</sup> mice, ICAM1 expression was enhanced in tumor vessels and there was an increased prevalence of intratumoral CD8<sup>+</sup> T cells after PD-1 blockade. This suggests that tumor endothelial cells in ELTD1<sup>-/-</sup> mice are more sensitive to inflammatory activation such as pro-inflammatory signaling induced by PD-1 blockade, enhancing expression of molecules that increase T-cell recruitment and a suppression of tumor growth.

Collectively, our results suggest that targeting ELTD1 may improve vessel function, which can lead to normalization of the tumor microenvironment, enhanced recruitment of T cells and increased transportation of anti-tumor drugs. Specifically, our data support targeting of ELTD1 in combination with cancer immunotherapy, and encourage further work focused on establishing efficient therapeutic options for ELTD1 inhibition in glioma.

## Supplementary Material

Supplementary material is available at *Neuro-Oncology* online.

## Keywords

ADGRL4 | ELTD1 | glioma | immunotherapy | vascular normalization

## Funding

This study was supported by Cancerfonden (CAN 2017/502, 20 1008 PjF, 20 1010 UsF, CAN 2015/1216), Barncancerfonden (PR2018-0148), The Swedish Research Council (Dnr 2016-02495, Dnr. 2020-02563), Emil and Wera Cornells Stiftelse, National Natural Science Foundation of China (81702489, 81911530166), and Knut and Alice Wallenberg foundation (Dnr KAW2019.0088).

## Acknowledgments

We thank Prof. Eric Holland, Fred Hutchinson Cancer Research Center, for generously sharing the VEcadTRAP mice.



**Conflict of interest statement.** The authors declare no conflicts of interest.

**Authorship statement.** H.H. designed and performed research, collected, analyzed, and interpreted data, and wrote the manuscript; M.G., B.L., L.v.H., K.V., T.v.d.W., and M.R. performed research, collected, analyzed, and interpreted data; F.P. and M.B. contributed to tissue microarrays; A.S. contributed to tissue microarrays and interpreted data; C.B. produced ELTD1-deficient mice; L.Z., E.D., and P.U.M. interpreted data; L.H. and L.L.C. performed bioinformatic analysis; R.L. interpreted data and wrote the manuscript; A.D. designed research, interpreted data, wrote the manuscript, and supervised the study.

## References

- Louis DN, Ohgaki H, Wiestler OD, et al. The 2007 WHO classification of tumours of the central nervous system. *Acta Neuropathol.* 2007;114(2):97–109.
- Wen PY, Kesari S. Malignant gliomas in adults. *N Engl J Med.* 2008;359(5):492–507.
- Dimberg A. The glioblastoma vasculature as a target for cancer therapy. *Biochem Soc Trans.* 2014;42(6):1647–1652.
- Georganaki M, van Hooren L, Dimberg A. Vascular targeting to increase the efficiency of immune checkpoint blockade in cancer. *Front Immunol.* 2018;9:3081.
- Louis DN, Perry A, Reifenberger G, et al. The 2016 World Health Organization classification of tumors of the central nervous system: a summary. *Acta Neuropathol.* 2016;131(6):803–820.
- Brat DJ, Verhaak RG, Aldape KD, et al.; Cancer Genome Atlas Research Network. Comprehensive, integrative genomic analysis of diffuse lower-grade gliomas. *N Engl J Med.* 2015;372(26):2481–2498.
- Zhang L, He L, Lugano R, et al. IDH mutation status is associated with distinct vascular gene expression signatures in lower-grade gliomas. *Neuro Oncol.* 2018;20(11):1505–1516.
- Dieterich LC, Mellberg S, Langenkamp E, et al. Transcriptional profiling of human glioblastoma vessels indicates a key role of VEGF-A and TGF $\beta$ 2 in vascular abnormalization. *J Pathol.* 2012;228(3):378–390.
- Dusart P, Hallstrom BM, Renne T, Odeberg J, Uhlen M, Butler LM. A systems-based map of human brain cell-type enriched genes and malignancy-associated endothelial changes. *Cell Rep.* 2019;29(6):1690–1706 e1694.
- Nechiporuk T, Urness LD, Keating MT. ETL, a novel seven-transmembrane receptor that is developmentally regulated in the heart. ETL is a member of the secretin family and belongs to the epidermal growth factor-seven-transmembrane subfamily. *J Biol Chem.* 2001;276(6):4150–4157.
- Wallgard E, Larsson E, He L, et al. Identification of a core set of 58 gene transcripts with broad and specific expression in the microvasculature. *Arterioscler Thromb Vasc Biol.* 2008;28(8):1469–1476.
- Masiero M, Simões FC, Han HD, et al. A core human primary tumor angiogenesis signature identifies the endothelial orphan receptor ELTD1 as a key regulator of angiogenesis. *Cancer Cell.* 2013;24(2):229–241.
- Zalles M, Smith N, Ziegler J, et al. Optimized monoclonal antibody treatment against ELTD1 for GBM in a G55 xenograft mouse model. *J Cell Mol Med.* 2020;24(2):1738–1749.
- Ziegler J, Pody R, Coutinho de Souza P, et al. ELTD1, an effective anti-angiogenic target for gliomas: preclinical assessment in mouse GL261 and human G55 xenograft glioma models. *Neuro Oncol.* 2017;19(2):175–185.
- Ziegler J, Zalles M, Smith N, et al. Targeting ELTD1, an angiogenesis marker for glioblastoma (GBM), also affects VEGFR2: molecular-targeted MRI assessment. *Am J Nucl Med Mol Imaging.* 2019;9(1):93–109.
- Georganaki M, Ramachandran M, Tuit S, et al. Tumor endothelial cell up-regulation of IDO1 is an immunosuppressive feed-back mechanism that reduces the response to CD40-stimulating immunotherapy. *Oncimmunology.* 2020;9(1):1730538.
- Wesseling P, Capper D. WHO 2016 classification of gliomas. *Neuropathol Appl Neurobiol.* 2018;44(2):139–150.
- Heiman M, Schaefer A, Gong S, et al. A translational profiling approach for the molecular characterization of CNS cell types. *Cell.* 2008;135(4):738–748.
- Heiman M, Kulicke R, Fenster RJ, Greengard P, Heintz N. Cell type-specific mRNA purification by translating ribosome affinity purification (TRAP). *Nat Protoc.* 2014;9(6):1282–1291.
- Kim D, Pertea G, Trapnell C, Pimentel H, Kelley R, Salzberg SL. TopHat2: accurate alignment of transcriptomes in the presence of insertions, deletions and gene fusions. *Genome Biol.* 2013;14(4):R36.
- Zhou Y, Zhou B, Pache L, et al. Metascape provides a biologist-oriented resource for the analysis of systems-level datasets. *Nat Commun.* 2019;10(1):1523.
- Zhao Z, Zhang KN, Wang Q, et al. Chinese Glioma Genome Atlas (CGGA): a comprehensive resource with functional genomic data from Chinese glioma patients. *Genom Prot Bioinform.* 2021:S1672-0229(21)00045-0.
- Gusev Y, Bhuvaneshwar K, Song L, Zenklusen JC, Fine H, Madhavan S. The REMBRANDT study, a large collection of genomic data from brain cancer patients. *Sci Data.* 2018;5:180158.
- Langenkamp E, Zhang L, Lugano R, et al. Elevated expression of the C-type lectin CD93 in the glioblastoma vasculature regulates cytoskeletal rearrangements that enhance vessel function and reduce host survival. *Cancer Res.* 2015;75(21):4504–4516.
- Scholz A, Harter PN, Cremer S, et al. Endothelial cell-derived angiopoietin-2 is a therapeutic target in treatment-naive and bevacizumab-resistant glioblastoma. *EMBO Mol Med.* 2016;8(1):39–57.
- Lugano R, Vemuri K, Yu D, et al. CD93 promotes  $\beta$ 1 integrin activation and fibronectin fibrillogenesis during tumor angiogenesis. *J Clin Invest.* 2018;128(8):3280–3297.
- Towner RA, Jensen RL, Colman H, et al. ELTD1, a potential new biomarker for gliomas. *Neurosurgery.* 2013;72(1):77–90; discussion 91.
- Batchelor TT, Gerstner ER, Emblem KE, et al. Improved tumor oxygenation and survival in glioblastoma patients who show increased blood perfusion after cediranib and chemoradiation. *Proc Natl Acad Sci U S A.* 2013;110(47):19059–19064.
- Gerstner ER, Emblem KE, Chang K, et al. Bevacizumab reduces permeability and concurrent temozolomide delivery in a subset of patients with recurrent glioblastoma. *Clin Cancer Res.* 2020;26(1):206–212.
- Lee S, Chen TT, Barber CL, et al. Autocrine VEGF signaling is required for vascular homeostasis. *Cell.* 2007;130(4):691–703.
- Phoenix TN, Patmore DM, Boop S, et al. Medulloblastoma genotype dictates blood brain barrier phenotype. *Cancer Cell.* 2016;29(4):508–522.
- Veys K, Fan Z, Ghobrial M, et al. Role of the GLUT1 glucose transporter in postnatal CNS angiogenesis and blood-brain barrier integrity. *Circ Res.* 2020;127(4):466–482.
- Honda M, Nakagawa S, Hayashi K, et al. Adrenomedullin improves the blood-brain barrier function through the expression of claudin-5. *Cell Mol Neurobiol.* 2006;26(2):109–118.

34. Wilhelm K, Happel K, Eelen G, et al. FOXO1 couples metabolic activity and growth state in the vascular endothelium. *Nature*. 2016;529(7585):216–220.
35. Favara DM, Zois CE, Haider S, et al. ADGRL4/ELTD1 silencing in endothelial cells induces ACLY and SLC25A1 and alters the cellular metabolic profile. *Metabolites*. 2019;9(12):287.
36. Pober JS, Merola J, Liu R, Manes TD. Antigen presentation by vascular cells. *Front Immunol*. 2017;8:1907.
37. Walch JM, Zeng Q, Li Q, et al. Cognate antigen directs CD8<sup>+</sup> T cell migration to vascularized transplants. *J Clin Invest*. 2013;123(6):2663–2671.